ORGANIC LETTERS

2009
Vol. 11, No. 14
2992−2995

Water-Soluble Rhamnose-Coated Fe_3O_4 Nanoparticles

Lenaic Lartigue,[†,‡] Khalid Oumzil,[§] Yannick Guari,[*,†] Joulia Larionova,[†] Christian Guérin,[†] Jean-Louis Montero,[*,§] Veronique Barragan-Montero,[§] Claudio Sangregorio,[*,‡] Andrea Caneschi,[‡] Claudia Innocenti,[‡] T. Kalaivani,[||,⊥] P. Arosio,[||] and A. Lascialfari[*,||,⊥,#]

Institut Charles Gerhardt Montpellier, UMR 5253 CNRS-UM2, Chimie Moléculaire et Organisation du Solide, Université Montpellier II, Place E. Bataillon, 34095 Montpellier cedex 5, France, Institut des Biomolécules Max Mousseron, UMR 5247, CNRS-UM1-UM2, Bâtiment de Recherche Max Mousseron, Ecole Nationale Supérieure de Chimie de Montpellier, 8 rue de l'Ecole Normale, 34296 Montpellier Cedex, France, INSTM Research Unit-Dipartimento di Chimica, Università di Firenze, via della Lastruccia 3, 50019 Sesto F.no Firenze, Italy, Istituto di Fisiologia Generale e Chimica Biologica, Università degli Studi di Milano, I-20134 Milano, Italy, CNR-INFM-S3 NRC, I-41100 Modena, Italy, and Dipartimento di Fisica "A. Volta" and CNR-INFM, Università degli studi di Pavia, Via Bassi 6, I-27100 Pavia, Italy

yannick.guari@univ-montp2.fr; jean-louis.montero@univ-montp2.fr; claudio.sangregorio@unifi.it; alessandro.lascialfari@unimi.it

Received May 11, 2009

ABSTRACT

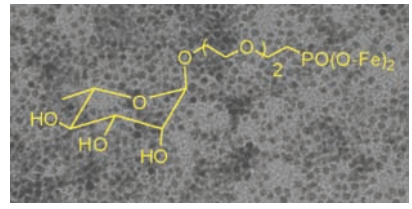

Water-soluble biocompatible rhamnose-coated Fe_3O_4 nanoparticles of 4.0 nm are obtained by covalent anchorage of rhamnose on the nanoparticles surface via a phosphate linker. These nanoparticles present superparamagnetic behavior and nuclear relaxivities in the same order of magnitude as Endorem that make them potential magnetic resonance imaging (MRI) contrast agents of a second generation, where the saccharides represent also specific ligands able to target lectins on skin cells.

Nanometer-scale magnetic nanoparticles have attracted a great deal of attention due to their unique properties and their potential applications in many fields including magnetic memory devices,[1] magnetic separations,[2] biotechnology, and biomedicine.[3] In particular, water-soluble and coated with various hydrophilic biocompatible molecules, iron oxide nanoparticles can be well stabilized in biological systems and used as contrast agents for magnetic resonance imaging (MRI).[4] Along this line, numerous works have been devoted to investigations on Fe_3O_4 nanoparticles stabilized with different biocompatible ligands including various polymers,[5] albumin,[6] folic acid,[7] dextran,[8] pluronic,[9]

[†] Université Montpellier II.
[‡] Università di Firenze.
[§] Ecole Nationale Supérieure de Chimie de Montpellier.
[||] Università degli Studi di Milano.
[⊥] CNR-INFM-S3 NRC.
[#] Università degli studi di Pavia.

(1) (a) Jun, Y.-W.; Choi, J.-S.; Cheon, J. *Chem. Commun.* **2007**, 1359. (b) Fanciuli, M.; Perego, M.; Bonafos, C.; Mouti, A.; Schamm, S.; Benassayag, G. *Adv. Sci. Tech.* **2006**, 156.

(2) (a) Latham, A. H.; Williams, M. E. *Acc. Chem. Res.* **2008**, *41*, 411. (b) Xu, C.; Sun, S. *Polym. Int.* **2007**, *56*, 821.

(3) Jun, Y.-W.; Seo, J.-W.; Cheon, J. *Acc. Chem. Res.* **2008**, *41*, 179.

(4) (a) Di Marco, M.; Sadun, C.; Port, M.; Guilbert, I.; Couvreur, P.; Dubernet, C. *Int. J. Nanomed.* **2007**, *2*, 609. (b) Corot, C.; Robert, P.; Idee, J. M.; Port, M. *Adv. Drug Delivery Rev.* **2006**, *58*, 1471. (c) Laurent, S.; Forge, D.; Port, M.; Roch, A.; Robic, C.; Elst, L. V.; Muller, R. N. *Chem. Rev.* **2008**, *108*, 2064.

10.1021/ol900949y CCC: $40.75
Published on Web 06/22/2009

starch,[10] herceptin,[11] nucleic acid molecules (aptamer),[12] peptides (cRGDyK),[13] and others. These investigations impressively show that the magnetic properties and contrast enhancement capacity of nanoparticles is strongly determined by various parameters, such as core and overall size, surface state properties, and degree of aggregation. Besides, the nature of the stabilizing ligand is also important for several reasons: (i) uncoated iron oxide nanoparticles are usually recognized and immediately eliminated from the body while surface modified nanoparticles present increased circulation time, which depends on the anchored ligand; (ii) the coated ligand increases the biocompability of the nanoparticles; (iii) ligands bearing active functionality such as a targeting moiety for desired receptors enhance selective nanoparticles transport to the cell membrane. Therefore, the design of iron oxide nanoparticles displaying appropriate magnetic properties coated with ligands able to target specific cells is needed to produce a new generation of nanoprobes for early diagnosis via MRI.

Among the biocompatible and cell-targeting ligands, saccharides are promising molecules for delivery of contrast agents to tumor cells. They are involved as recognition markers in numerous physiological and pathological processes, mainly occurring on the cell surfaces and may be recognized by carbohydrate-binding proteins, like antibodies, enzymes, and lectins. Moreover, membrane-bound receptors, like lectins, assist internalization of material inside the cell via endocytosis upon the binding of their ligand.[14] Few examples of iron oxide nanoparticles coated with saccharide molecules have been previously given, consisting in the attachment of dihydroxyborylphenyl groups to magnetite nanoparticles and complexation of the former with different mono- and oligosaccharides,[15] the grafting of silica-coated magnetite nanoparticles with functionalized D-mannose through a triazol linker,[16] the noncovalent coating of the magnetite nanoparticles with poly(D,L-lactide-*co*-glycoside) via emulsion techniques,[17] or the coprecipitation of iron salts in the presence of D-mannose.[18] However, these methods present several drawbacks: (i) the difficulty in the coating process control may produce a multilayer coating giving heterogeneous samples, which is especially accentuated in the case of noncovalent linkages of saccharides with nanoparticles; (ii) dimers or trimers of nanoparticles may be encapsulated in the same shell; and (iii) the last method suffers the lack of good size control of the particles.

In this communication, we report a new approach to achieve size-controlled water-soluble magnetic Fe_3O_4 nanoparticles covalently coated with monosaccharide molecules linked via a phosphonate moiety. For the first time, a phosphonate linkage, known for its stability toward enzymes, was used for the preparation of coated nanoparticles with carbohydrates. As for the carbohydrate, we focused our study on rhamnose encouraged by previous results obtained with this sugar. Indeed, in recent work, it was shown that liposomes containing a fluorescent substance could transfer this fluorescence to skin cells provided that the liposomal membrane contained a rhamnose ligand. Moreover, *ex vivo* experiments on human skin section demonstrated specific delivery to the epidermis or the horny layer due to the presence of rhamnose-ligands on the surface of liposomes.[19] For those reasons, we wish to develop the use of this sugar for the targeting of human skin cells.

Scheme 1. Synthesis of (a) the Phosphonate-Bearing Rhamnose and (b) the Rhamnose-Coated Fe_3O_4 Nanoparticles

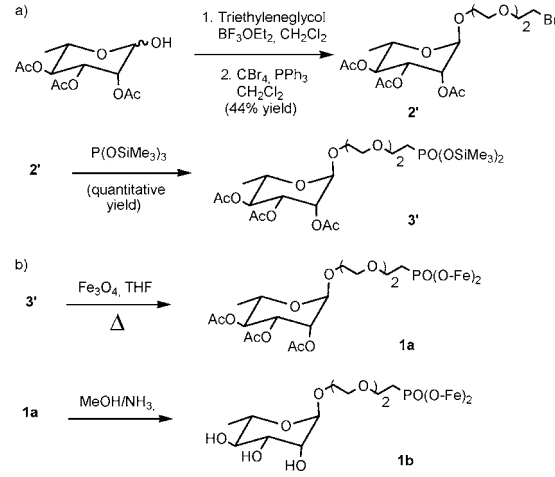

The synthesis of the sugar functionalized at the anomeric position depicted in Scheme 1a was carried out in five steps, leading mainly to the α-anomers (95/5). The hydroxyl protection was obtained by the action of acetic anhydride in pyridine. The hydrazinium acetate allowed deprotecting selectively for the anomeric position.[20] The glycosylation, of the deprotected sugar, by the TEG moiety was obtained in an excellent yield using boron trifluoride as catalyst. Primary alcohol was then halogenated by the couple triphenylphosphine/carbon tetrachloride, and

(5) Yang, J.; Lee, T. I.; Lim, E.-K.; Hyung, W.; Lee, C.-H.; Song, Y. J.; Suh, J.-S.; Yoon, H.-G.; Huh, Y.-M.; Haam, S. *Chem. Mater.* **2007**, *19*, 3870.
(6) Renshaw, P. F.; Owen, C. S.; McLaughlin, A. C.; Frey, T. G.; Leigh, J. S. *Magn. Reson. Med.* **1986**, *3*, 217.
(7) (a) Yang, X.; Chen, Y.; Yuan, R.; Chen, G.; Blanco, E.; Gao, J.; Shuai, X. *Polymer* **2008**, *49*, 3477. (b) Shi, X.; Wang, S. E.; Swanson, S. D.; Ge, S.; Cao, Z.; Van Antwerp, M. E.; Landmark, K. J.; Baker, J. R., Jr. *Adv. Mater.* **2008**, *20*, 1671. (c) Wang, S. H.; Shi, X.; Van Antwerp, M.; Cao, Z.; Swanson, S. D.; Bi, X.; Baker, J. R., Jr. *Adv. Mater.* **2007**, *17*, 3043.
(8) (a) Shen, T.; Weissleder, R.; Papisov, M.; Bogdanov, A.; Brady, T. J. *Magn. Reson. Med.* **1993**, *29*, 599. (b) Reimer, P.; Jahnke, N.; Schima, M.; Deckers, F.; Marx, F.; Holzknecht, N.; Saini, S. *Radiology* **2000**, *217*, 152. (c) Zhao, M.; Kircher, M. F.; Josephson, L.; Weissleder, R. *Bioconjugate Chem.* **2002**, *13*, 840.
(9) (a) Thunemann, A. F.; Schutt, D.; Kaufner, L.; Pison, U.; Mohwald, H. *Langmuir* **2006**, *22*, 2351. (b) Jain, T. K.; Morales, M. A.; Sahoo, S. K.; Leslie-Pelecky, D. L.; Labhasetwar, V. *Mol. Pharmaceutics* **2005**, *2*, 194.
(10) Kim, D. K.; Mikhaylova, M.; Wang, F. H.; Kehr, J.; Bjelke, B.; Zhang, Y.; Tsakalakos, T.; Muhammed, M. *Chem. Mater.* **2003**, *15*, 4343.
(11) Huh, Y.-M.; Jun, Y.-W.; Song, H.-T.; Kim, S.; Choi, J.-S.; Lee, J.-H.; Yoon, S.; Kim, K.-S.; Shin, J.-S.; Suh, J.-S.; Cheon, J. *J. Am. Chem. Soc.* **2005**, *127*, 12387.
(12) Yigit, M. V.; Mazumdar, D.; Lu, Y. *Bioconjugate Chem.* **2008**, *19*, 412.
(13) Xie, J.; Chen, K.; Lee, H.-Y.; Xu, C.; Hsu, A. R.; Peng, S.; Chen, X.; Sun, S. *J. Am. Chem. Soc.* **2008**, *130*, 7542.
(14) Barragan, V.; Menger, F. M.; Caran, K.; Vidil, C.; Morere, A.; Montero, J.-L. *Chem. Commun.* **2001**, *1*, 85.
(15) Shimomura, M.; Ono, B.; Oshima, K.; Miyauchi, S. *Polymer* **2006**, *47*, 5785.
(16) El-Boubbou, K.; Gruden, C.; Huang, X. *J. Am. Chem. Soc.* **2007**, *129*, 13393.

an Arbuzov reaction with the sorting-trimethylsilyl phosphite[21] led to the desired phosphonate. The monodisperse Fe_3O_4 nanoparticles coated with oleic acid and oleyl amine of the size 3.8(0.6) nm were synthesized using a previously published procedure.[22] Strong binding of phosphonate with Fe was demonstrated previously.[23] The postsynthetic anchorage of the phosphonate-functionalized rhamnose to the surface of the Fe_3O_4 nanoparticles in order to obtain rhamnose-functionalized Fe_3O_4 nanoparticles, **1a**, was performed in THF with heating for 24 h and then the deprotection of the rhamnose acetate groups was performed in a methanol/ammonia mixture in order to give sample **1b** (see Scheme 1b). While the starting iron oxide nanoparticles are nonsoluble in methanol and water, nanoparticles **1a** are soluble in methanol but still not soluble in water and nanoparticles **1b** are fully soluble in water in agreement with the organic groups present on the surface of the nanoparticles for each step. Following this synthetic strategy, the rhamnose moiety was covalently bound to the Fe_3O_4 nanoparticles via the phosphonate moiety which precludes rhamnose leaching and formation of uncoated Fe_3O_4 nanoparticles in the living organism. Such assessment was verified by submitting an aqueous solution of the iron oxide nanoparticles at physiological pH under intense sonication followed by precipitation and intense washing to remove all improperly anchored organic molecules from the nanoparticles surface. IR analysis performed after such treatment still showed the presence of the Rhamnose-phosphonate molecule, and the EDX analysis performed showed an unchanged Fe/P ratio confirming the absence of Rhamnose-phosphonate release after such harsh treatment. Furthermore, it ensures presence of rhamnose moieties pointing out from the iron oxide nanoparticles for optimum recognition process toward the appropriate lectin and cell internalization. The infrared spectrum of sample **1a** in comparison to the spectrum of the Fe_3O_4 nanoparticles coated with oleic acid and oleyl amine showed the appearance of strong bands at 1747 and 1226 cm^{-1} attributed to the stretching elongation of ν(COO) and ν(CO) along with the bands at 1080 and at 1051 cm^{-1} assigned to ν(COC) and $\nu(CH_{cycle})$, respectively (Figure 1S, Supporting Information).[23] The weak band of the ν(P−O−Fe) mode appears at 984 cm^{-1}, indicating anchoring of at least one phosphonate moiety to the surface (Figure 1Sb, Supporting Information).[23a] On the other hand, the usually observed shoulders of the second ν(P−O−Fe) band at 1015 cm^{-1} attributed to the presence of a bidentate mode of coordination of phosphonate to the surface of nanoparticles are not well visible. For this reason, we cannot state if the phosphonate group presents monodentate or bidentate mode of coordination. The characteristic broad envelop at 588 cm^{-1} attributed to ν(Fe−O) bands of Fe_3O_4 was preserved, indicating the preservation of Fe_3O_4 after rhamnose anchorage. For sample **1b**, after deprotection of the rhamnose acetate groups, the band at 1747 cm^{-1} (ν(COO)) completely disappears and the intensity of the band at 1226 cm^{-1} (ν(CO)) is strongly decreased (Figure 1S, Supporting Information). The powder X-ray diffraction pattern within the range of 2θ (30−60°) of **1b** exhibits diffraction peaks indexed as (220), (311), (400), (422), (511), and (440) reflections, characteristics of the cubic structure of magnetite Fe_3O_4 (Figure 2S, Supporting Information).

The transmission electronic microscopy (TEM) measurements performed for the nanoparticles show the presence of spherical nonaggregated uniform nanoparticles homogeneously dispersed in water. The TEM image of the nanoparticles **1b** is shown in Figure 1 as a representative example. The size

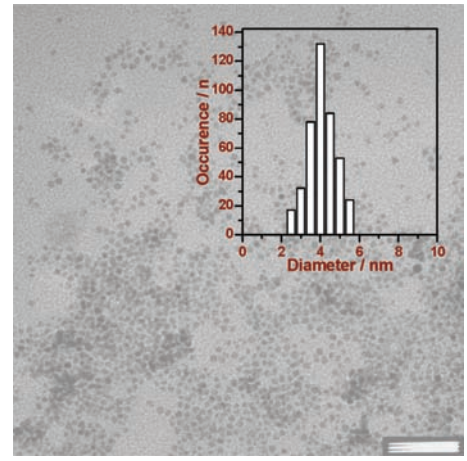

Figure 1. TEM image of sample **1b**.(Inset) Size distribution histogram. Scale bar = 50 nm.

distribution as obtained from TEM measurements shows that the mean size value of the nanoparticles **1b** is centered at 4.1 (0.7) nm (inset of Figure 1) whereas for nanoparticles **1a** it is centered at 4.0 (0.7) nm (Figure 3S, Supporting Information), indicating that no change in the nanoparticles size is occurring after acetate groups removal on rhamnose. The dynamic light scattering measurements of the hydrodynamic size of the nanoparticles **1b** give the value of 8.2 (1.3) nm.

The magnetic properties of the nanoparticles were studied in direct current (dc) and alternating current (ac) modes. Figure 2 shows the zero field-cooled (ZFC)/field-cooled (FC) magnetization curves in the range of 2−70 K measured for sample **1b**.

For the ZFC experiment, the sample is cooled in zero field and then heated in a field of 5 mT while the net magnetization of the sample is recorded. The FC data are obtained by cooling the sample under the same magnetic field of 5 mT after the ZFC experiments and recording the change in net sample magnetization with temperature. The ZFC curve shows a narrow peak at 17 K, indicating the blocking temperature of nanoparticles with mean size. The FC and ZFC curves coincide at high

(17) Astete, C. E; Kumar, C. S. S. R.; Sabilov, C. M. *Coll. and Surf. A: Physicochem. Eng. Aspects* **2007**, *299*, 209.
(18) Horac, D.; Babic, M.; Jendelova, P.; Herynek, V.; Trchova, M.; Pientka, Z.; Pollert, E.; Sykova, E. *Bioconjugate Chem.* **2007**, *18*, 635.
(19) (a) Barragan-Montero, V.; Winum, J.-Y.; Molès, J.-P.; Juan, E.; Clavel, C.; Montero, J.-L. *Eur. J. Med. Chem.* **2005**, *40*, 1022. (b) Barragan, V.; Montero, J.-L.; Winum, J.-Y.; Juan, E.; Moles, J.-P. French Patent FR 2854896, 2007.
(20) Michaëlis, A.; Becker, T. *Chem. Ber.* **1897**, *30*, 1003.
(21) Montero, J.-L.; Imbach, J. L. *Eur. J. Med. Chem.* **1982**, *17*, 97.
(22) Sun, S.; Zeng, H *J. Am. Chem. Soc.* **2004**, *126*, 273.
(23) (a) Barja, B. C.; Tejedor-Tejedor, M. I.; Anderson, M. A. *Langmuir* **1999**, *15*, 2316–2321. (b) Yee, C.; Kataly, G.; Ulman, A.; Prozorov, T.; White, H.; King, A.; Rafailovich, M.; Sokolov, J.; Gedanken, A. *Langmuir* **1999**, *15*, 7111.

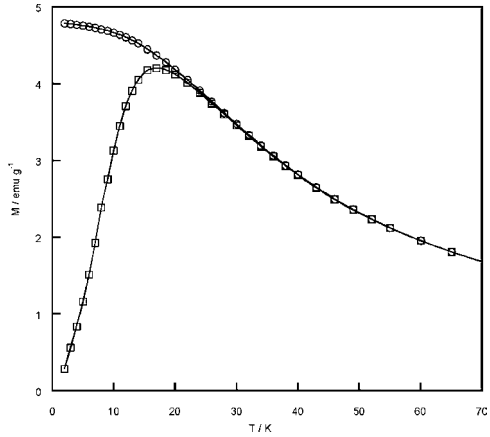

Figure 2. Zero field cooled (ZFC) (□)/field cooled (FC) (○) magnetization curves for the sample **1b** recorded with an applied field of 5 mT.

temperatures and start to separate at 20 K, indicating the blocking temperature of the largest particles. The closeness of the blocking temperature and the temperature of the ZFC/FC curves separation indicates the presence of nanoparticles with a narrow size distribution.[24] To investigate the nature of the irreversibility observed in FC/ZFC curves in more detail, we measured the temperature dependence of the in-phase (χ') and the out-of-phase (χ'') components of the ac susceptibility (Figure 4S, Supporting Information). At 70 Hz, χ' and χ'' exhibit a peak at ~25 K and ~14 K, respectively, which shift toward higher temperature with increasing frequency. The temperature dependence of the relaxation time extracted from the maximum of the χ" component of the ac susceptibility could be fit to an Arrhenius law, $\tau = \tau_0 \exp(E_a/k_BT)$, where E_a is the average energy barrier for the reversal of the magnetization, τ_0 is the attempt time and k_B is the Boltzmann constant. According to the Néel model, this law governs the temperature dependence of the relaxation of the magnetization of noninteracting superparamagnetic systems.[25] The values of the energy barrier, E_a/k_B, and of the pre-exponential factor, τ_0, are equal to 260(8) K and 1.68×10^{-11} s, respectively (inset of Figure 4S, Supporting Information). Thus, the as-obtained nanoparticles present a pure superparamagnetic regime that enables to consider them as potential T_2 contrast agent.

The ^{1}H NMR relaxometry characterization (i.e., NMR-Dispersion profile) of sample **1b** was performed at room temperature by measuring the longitudinal and the transverse nuclear relaxation times T_1 and T_2, in the frequency range 10 kHz $\leq \nu \leq$ 65 MHz for T_1 and 15 MHz $\leq \nu \leq$ 60 MHz for T_2.[26] It should be noticed that the measurements at room and physiological temperatures gave the same results within 10%. The efficiency of the MRI contrast agents is determined by measuring the nuclear relaxivities $r_{1,2}$ defined as $r_i = [\,(1/T_i)_{meas} - (1/T_i)_{dia}\,]/c$ ($i = 1,2$) where $(1/T_i)_{meas}$ is the value measured for the sample with concentration c (mmol L^{-1}) of magnetic center (0.649 mmol L^{-1} of Fe in our case), and $(1/T_i)_{dia}$ refers to the nuclear relaxation rate of the diamagnetic host solution (water in our case). Figure 3 reports the r_2 and r_1 values for the

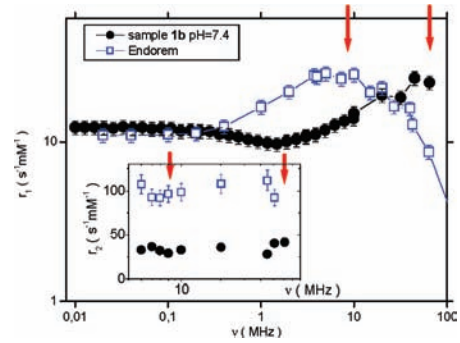

Figure 3. Spin−lattice (main picture) and spin−spin (inset) relaxivity of sample **1b**, collected at $t \approx 25$ °C, compared to the same quantity reported for the commercial compound Endorem. The lines connecting the experimental points are guides to the eye, whereas the arrows indicate approximately the working frequencies of the most diffused clinical MRI imagers (0.2 T and 1.5 T).

sample **1b**, together with the values for Endorem, as a function of the measuring frequency. As can be easily seen, the relaxivities of our sample are not much lower than the one of Endorem, indicating that our nanoparticles may be considered as an efficient contrast agent, and, in addition, with bound vectors (saccharides) allowing to implement molecular imaging when addressed to specific cells.

In summary, water-soluble biocompatible rhamnose-coated Fe_3O_4 nanoparticles of *ca.* 4.0 nm were obtained by the organic phase covalent anchorage of acetate-protected rhamnose on the nanoparticles surface via a -PO(OSiMe$_3$)$_2$ moiety and the subsequent removal of the acetate protecting groups. In comparison to the previously published nanoparticles coated with other saccharide molecules, the present nanoparticles are monodispersed, size controlled and present good stability due to the covalent anchorage of rhamnose to the surface of the nanoparticles. They present superparamagnetic behavior and nuclear relaxivities comparable with Endorem. These results certify that our approach is a promising way toward a new family of superparamagnetic MRI contrast agents of a second generation which are designed for the specific targeting of cells.

Acknowledgment. We thank Mme Corine Reibel (Institut Charles Gerhardt, Montpellier, France) for magnetic measurements. We also thank the CNRS, the Université Montpellier II and the European Network of Excellence Magmanet (NMP3-CT-2005-515767) for financial support. L.L. thanks the UFI (GF/IR/732/07, n°25) for financial support. Thanks are due to M. Mariani for help in experimental measurements.

Supporting Information Available: Experimental procedures and spectroscopic data for all compounds and magnetic nanoparticles characterization. This material is available free of charge via the Internet at http://pubs.acs.org.

OL900949Y

(24) Bonacchi, D.; Caneschi, A.; Dorignac, D.; Falqui, A.; Gatteschi, D.; Rovai, D.; Sangregorio, C.; Sessoli, R. *Chem. Mater.* **2004**, *16*, 2016.
(25) Nèel, L. *Adv. Phys.* **1955**, *4*, 191.
(26) Ferrante, G.; Sykora, S. *Adv. Inorg. Chem.* **2005**, *57*, 405.